CARBON letters

Original Articles
Carbon Letters Vol. 20, 47-52 (2016)

Activating needle coke to develop anode catalyst for direct methanol fuel cell

Young Hun Park[1], Ui-Su Im[2], Byung-Rok Lee[3], Dong-Hyun Peck[3], Sang-Kyung Kim[3], Young Woo Rhee[1,♠] and Doo-Hwan Jung[2,3,♠]

[1]Department of Energy Science and Technology, Graduate School of Energy Science and Technology, Chungnam National University, Daejeon 34134, Korea
[2]Advanced Energy Technology, University of Science and Technology, Daejeon 34113, Korea
[3]New & Renewable Energy Research Division, Korea Institute of Energy Research, Daejeon 34129, Korea

Article Info

Received 26 March 2016
Accepted 23 May 2016

♠Corresponding Author
E-mail: doohwan@kier.re.kr
ywrhee@cnu.ac.kr
Tel: +82-42-860-3577
+82-42-821-5688

Open Access

DOI: http://dx.doi.org/10.5714/CL.2016.20.047

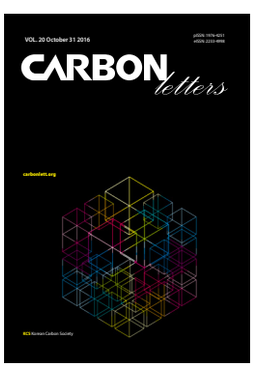

http://carbonlett.org

pISSN: 1976-4251
eISSN: 2233-4998

Abstract

Physical and electrochemical qualities were analyzed after KOH activation of a direct methanol fuel cell using needle coke as anode supporter. The results of research on support loaded with platinum-ruthenium suggest that an activated KOH needle coke container has the lowest onset potential and the highest degree of catalyst activity among all commercial catalysts. Through an analysis of the CO stripping voltammetry, we found that KOH activated catalysis showed a 21% higher electrochemical active surface area (ECSA), with a value of 31.37 m^2/g, than the ECSA of deactivated catalyst (25.82 m^2/g). The latter figure was 15% higher than the value of one specific commercial catalyst (TEC86E86).

Key words: needle coke, activated carbon, porous carbon, surface areas

1. Introduction

Faced with the problems of the depletion of fossil energy and increasing environmental pollution, researchers are putting fuel cells in the spotlight as an alternative energy source for the future. Fuel cells are environmentally-friendly and have a long life [1,2]. Fuel cells can be made using an inverse water electrolysis reaction, in which an electric cell generates a direct current by combining the hydrogen in the fuel and oxygen in the air into electrical energy through an electrochemical redox-reaction. As the fuel is directly changed into electrical energy, its energy conversion efficiency is higher than that possible when using existing generating devices. In addition, as long as the fuel is supplied, the cell can continue to generate energy, and has lower impact on the environment in terms of air contaminants (such as NO_x and So_x), because they are not emitted during operation of fuel cells. Moreover such devices are inclined to be less noisy. For these reasons, fuel cells have been intensively researched for use in military and leisure applications, as power supply for robotic automation and precision instruments, and in the transportation and aerospace defense industries, including high-tech aircraft and rockets or missiles [3].

A recent trend shows that studies are beginning to focus on polymer electrolyte membrane fuel cells, which use hydrogen as a fuel, and direct methanol fuel cells (DMFCs) which use methanol as a fuel. DMFCs have the following strengths: the methanol used as fuel has a high energy density (hydrogen 658 kcal/L and methanol 3800 kcal/L); device production costs are low; and the supply and transport is easy. At the same time, because no fuel reforming device is necessary thanks to the structure of the system, the system can be miniaturized, which has propelled DMFCs into the

limelight for use in next-generation mobile devices. Due to these advantages, DMFCs are receiving attention as an optimal power source that could be used to replace primary and secondary cells, which emit environmental pollution when discarded [4,5].

For the commercialization of DMFCs, fewer crossovers in the methanol and higher activity of the catalysts are required [6]. Especially, Pak et al. [7] have pointed out the cost problem and the problem of activity degradation due to CO-deposited platinum film, as shortcomings of the excessive use of an expensive platinum catalyst [8].

To enhance the efficiency of the usage of Pt, Nam et al. [9] have suggested that a support made by the template method could enhance the catalytic activity so that active carbon, which is mesoporous, could increase the oxidation speed of the methanol [10].

Ryoo et al. [11] produced sets of porous carbons by combining carbon precursor with various types of silica, carbonizing the mixture, and then etching the silica at the end of the process. Chai et al. [12] used phenol and formaldehyde as carbon precursor, mixing these materials and carbonizing them with silica to produce porous carbons, which were then used as catalyst support. As a result, the process of methanol oxidation became more active. Qiao et al. [13] observed improved electric conductivity followed by the increase of specific surface area of a device that utilized activated carbon produced through KOH activation with needle coke [14-17].

Therefore, in this research, porous support was produced with needle coke, into which platinum-ruthenium was loaded. The activation of the anode catalyst was then examined. The structural chemical qualities of the support and the catalyst were examined using a set of procedures including energy dispersive X-ray spectroscopy (EDS) and X-ray diffraction (XRD). Methods such as cyclic voltammetry (CV), methanol oxidation, and CO stripping voltammetry were applied to analyze the electrochemical active surface area (ECSA) and the activation of the catalyst during methanol oxidation.

2. Experimental

2.1. Production of catalyst support

The catalyst support that was used in the research was made with needle coke produced by refining coal tar (POSCO Chemtech Co., Seoul, Korea), by heat processing it at 500°C. The structural quality of the needle coke is shown in Fig. 1.

Fig. 2 shows the production procedure for the catalyst support. The needle coke was pulverized three times (30 min/set), into 100–150 μm sized particles; then powder was combined with KOH and activated for 1 h at 800°C using nitrogen gas as a carrier. After the activation, the product was made into porous activated carbon, neutralized with HCl, and washed with distilled water. Then it was dehydrated for 24 h at 110°C.

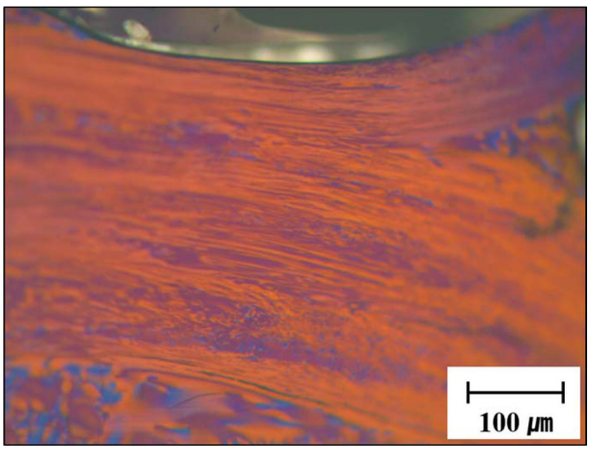

Fig. 1. Polarization microscope analysis images of anisotropic textures of needle coke.

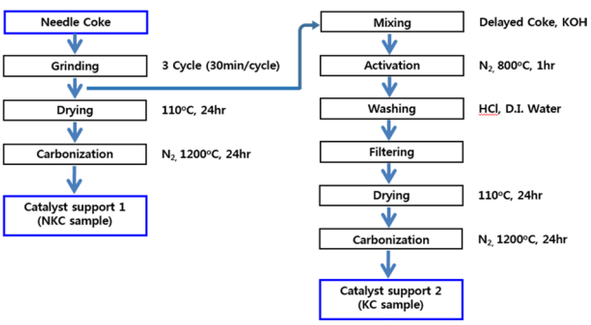

Fig. 2. Schematic diagram for the preparation of porous carbon from needle coke.

2.2. Catalyst loading

The catalyst was loaded into the carbonized powder coke support and KOH activated needle-shaped carbon support using $H_2PtCl_6 \cdot H_2O$ (Aldrich) and $RuCl_3 \cdot 3H_2O$ (Aldrich) as the catalyst precursors. To load the catalyst, suitable amounts of ultrapure water and activated carbon were put into an ultrasonic generator for 30 min and agitated for 12 h. The mixture was agitated with the catalyst precursor mixture of $H_2PtCl_6 \cdot H_2O$ (Aldrich) and $RuCl_3 \cdot 3H_2O$ (Aldrich), dissolved in water at a 1:1 mole ratio for 24 h. Then it was loaded with the metal catalyst (0.5 M $NaBH_4$) using the reduction method [18]. The catalysts loaded into the activated carbon were washed with distilled water for 3 h and dehydrated for 24 h at 80°C to produce a 60 wt% Pt-Ru/porous carbon anode catalyst.

2.3. Analysis of shape and electrochemical quality of the catalyst

The pore distribution and specific area of the produced catalyst were analyzed with a BELSORP-mini II (Microtrac). The specific area was calculated using the Vm value with the slope and the intercept values as determined using the Brunauer-Em-

Table 1. The Pt/Ru ratio measured by EDS as a function of Pt/Ru ratio in the precursor

Sample	Pt:Ru in precursors (wt%)		Pt:Ru in samples (wt%)	
	Pt	Ru	Pt	Ru
NKC-PtRu/C	70	30	68.82	31.18
KC-PtRu/C	70	30	69.27	30.73

EDS, energy dispersive X-ray spectroscopy; NKC, non-KOH activated carbon; KC, KOH activated carbon.

mett-Teller (BET) method. The volume and size of the pores were examined using the Barrett-Joyner-Halenda (BJH) method, which is an application of the Kelvin method [19].

The crystallizability of the produced catalyst was examined by XRD (Dmax-2500pc; Rigaku) analysis, while the composition was determined by EDS analysis (Table 1). The methanol oxidation quality of the catalyst was examined by the CV method using an electrochemical examiner (PGSTAT204; Metrohm Autolab, Utrecht, the Netherlands). In this analysis, 0.5 M methanol was combined with 0.5 M H_2SO_4 and scanned at 50 mV/s. Ag/AgCl was used as a reference electrode, and a three-electrode system was employed as the Pt counter-electrode. The catalyst loaded into the activated carbon was mixed with Nafion and applied to glassy carbon. A drop of 10 μL catalyst ink was dehydrated. Potentiostat (AFCBP1; Pine Instrument Co., Grove City, PA, USA) was employed and the remaining oxygen was removed by purging nitrogen gas into a 30°C water jacket for 1 h while the 0.5 M H_2SO_4 was continuously replenished.

CO stripping was performed with 0.5 M H_2SO_4 aqueous solution and scanning at 50 mV/s under 0.0–1.0 V electric potential. We put carbon monoxide into the deoxidized aqueous solution so that the surface of the catalyst would absorb carbon monoxide atoms. To keep the carbon monoxide absorbed on the surface, we applied and maintained the same voltage and introduced nitrogen gas for 20 min to remove carbon monoxide gas in the solution so that we could proceed with the voltammetry method.

3. Results and Discussion

3.1. Analysis of the physical qualities of catalyst and support

Table 2 shows the results for the specific area, the total volume of pores, and the analysis of the mesoporous pores on the catalyst support-KOH activated needle coke. The results were obtained using a surface area measuring set (BELSORP-mini II; Microtrac). As can be seen in the table, the specific area of KOH increased from 101.1 m^2/g before treatment (non-KOH activated carbon or NKC), to 2560.6 m^2/g after treatment (KOH activated carbon or KC). The total volume of pores was measured and found to have increased approximately 10 times from 0.1263 to 1.4235 cm^3/g. In addition, the total volume of mesoporous pores increased about seven times from 0.1043 cm^3/g in the untreated sample to 0.7235 cm^3/g after treatment. These results suggest

Table 2. Structural parameters of non-KOH carbon treatment and KOH carbon treatment

Sample	Specific surface area (m^2/g)	Total pore volume (cm^3/g)	Mesopore volume (cm^3/g)
NKC	101.1	0.1263	0.1043
KC	2560.6	1.4235	0.7235

NKC, non-KOH activated carbon; KC, KOH activated carbon.

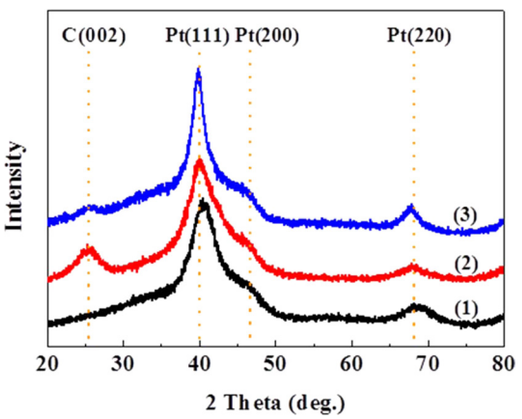

Fig. 3. X-ray diffraction patterns of the electrodeposited samples. (1) TANAKA-Pt-Ru/C, (2) NKC-Pt-Ru/C, and (3) KC-Pt-Ru/C. NKC, non-KOH activated carbon; KC, KOH activated carbon.

that KOH activation develops micro pores and mesoporous pores to a dramatic degree.

The results of XRD analysis for the catalyst in which Pt-Ru was loaded into active carbon are shown in Fig. 3. For comparison, we also analyzed the commercial catalyst-TANAKA PtRu/C (TEC86E86; TANAKA Holdings Co., Tokyo, Japan) under the same conditions. The results for this catalyst are shown in Fig. 3 as well. As can be seen in the figure, peaks at about 40°, 46°, and 68° (the characteristic peaks of FCC metal [111], [200], and [220]) could be observed for the PtRu/C loaded catalyst. The peak at 26°, which represents the crystallizability of carbon, suggests that the KC-PtRu/C and NKC-PtRuC catalysts were well crystallized compared to the Tanaka catalyst, which used carbon black as its support. KC-PtRu/C, in particular, showed the best carbon crystallizability. This is why needle coke became the primary carbon structure after heat treatment at 1200°C. However, when carbon was KOH activated, KC-PtRu/C showed lower crystallizability than that of NKC-PtRu/C because the KOH treatment caused the coke carbon structure to become amorphous. The same result has been reported in previous research by Qiao et al. [13].

3.2. Analysis of electrochemical quality

3.2.1. CV analysis of catalysts

CV was used not only to analyze the interaction between hydrogen and oxygen but also to examine the electrochemical stability. Fig. 4 shows the results of the CV analysis. Reaction

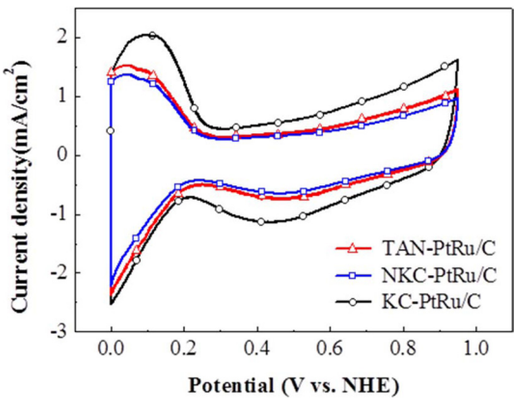

Fig. 4. Cyclic voltammogram of TANAKA-PtRu/C, NKC-PtRu/C, and KC-PtRu/C. Currents were normalized to the loading of metal. NKC, non-KOH activated carbon; KC, KOH activated carbon; NHE, normal hydrogen electrode.

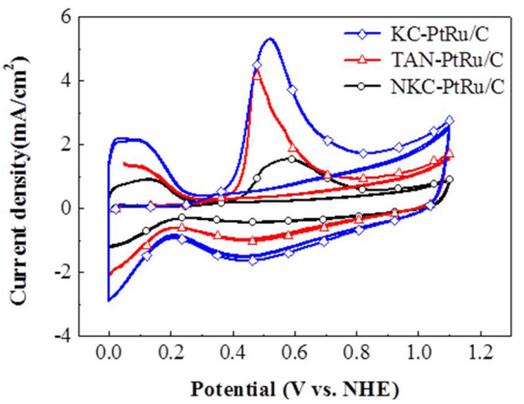

Fig. 5. CO stripping of the prepared catalysts. TANAKA-PtRu/C, NKC-PtRu/C, and KC-PtRu/C (electrolyte: 0.5 M H_2SO_4, 30°C, scan rate: 50 mV/s). NKC, non-KOH activated carbon; KC, KOH activated carbon.

peaks against absorption and desorption of H^+, were observed when we examined PtRu/C within the range of 0.0–0.2 V. In the range 0.6–0.8 V, H_2O dropped from $Pt(OH)_2$, which thereby became Pt-O, while O_2 was desorbed from H_2O within the range 0.8–1.0 V. Within the range 0.4–0.5 V, the cathodic current increased during the H^+ desorption of oxygen from Pt-O. CV was used not only to analyze the interaction between hydrogen and oxygen but also to examine the electrochemical stability.

The peaks of the current density are not only affected by the activation of the catalysts themselves but also by the surface area of activation. The ECSA of Pt in the catalysts can be determined using the measured hydrogen absorption area of the CV according to the following equation:

$$ECSA = \frac{Q_{H(mC)}}{Q_{Href_{(mC/gPt)}} \times M_{Pt_{(g/cm^2)}}}$$

In this formula, Q_H represents the quantity of electrical charge in the hydrogen oxidation reaction absorbed on the surface of Pt, M_{Pt} represents the mass of loaded Pt, and $Q_{H\ ref}$ is assumed to be 0.21 mC/cm² [20]. The calculated active surface areas are shown in Table 3. The results for TANAKA-PtRu/C, NKC-PtRu/C, and KC-PtRu/C were 22.34, 20.78, and 45.51 m²/g, respectively. KC-PtRu/C, which has the widest current density peak area, had the highest ECSA value; therefore, these results suggest that the current density and the active surface area are closely related.

3.2.2. CO Stripping analysis of catalysts

To examine the activity in carbon monoxide oxidation of the synthesized catalysts, CO stripping voltammetry analysis was conducted and the results are shown in the voltage current curve provided in Fig. 5. In the first cycle, a needle shaped oxidation peak can be observed within the range of 0.4–0.8 V. In the second cycle, a peak was observed for unabsorbed carbon monoxide. It can be inferred from these results that carbon monoxide absorbed on the surface of the catalyst was completely oxidized in the first cycle. The Pt surface area was calculated using the wide peak area within the range 0.4–0.8 V. The ECSA value can be found using the following equation with the quantities of electrical charge divided into two sections: Q_{co}-absorption and Q_{co}-desorption.

$$ECSA_{CO} = \frac{Q_{CO(mC)}}{0.42_{(mC/gPt)} \times Pt\ loading_{(g/cm^2)}}$$

The 0.42 (mC/gPt) value in the formula is known as the electrical charge value when hydrogen is absorbed in a single layer on the surface of platinum. Pt loading (g/cm²) indicates the quantity of platinum per unit area of the electrode. In this study, ECSA was calculated using the electrical charge value of CO desorption. As a result, the sizes of the surface areas were found to occur in the order of KC-PtRu/C > TANAKA-PtRu/C > NKC-PtRu/C (Table 3). KC-PtRu/C catalyst loaded into porous carbon had a wider effective surface area and higher activity than those characteristic of TANAKA-Pt/Ru/C, the commercial catalyst, or NKC-PtRu/C (the last of which is non-KOH activated).

3.2.3. Methanol oxidation reaction

To examine the stability of an electrode synthesized by methanol oxidation, the electrostatic potential of a 0.5 M

Table 3. Comparison of the TANAKA-PtRu/C, NKC-PtRu/C and KC-PtRu/C electrochemical properties

Sample	Particle size by XRD (nm)	ECSA by CV (m²/g)	ECSA by CO stripping (m²/g)	Onset potential (V)
TANAKA-PtRu/C	2.66	22.34	25.71	0.543
NKC-PtRu/C	2.61	20.78	13.07	0.571
KC-PtRu/C	2.69	45.51	32.54	0.515

XRD, X-ray diffraction; ECSA, electrochemical active surface area; CV, cyclic voltammetry; NKC, non-KOH activated carbon; KC, KOH activated carbon.

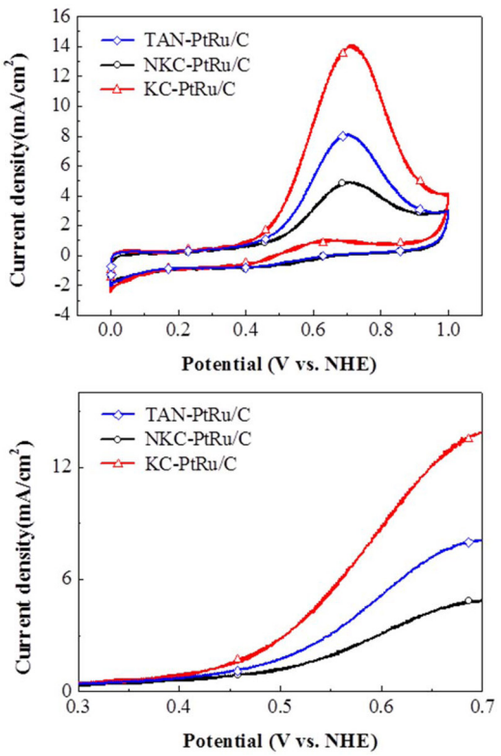

Fig. 6. Linear sweep voltammogram of catalysts. TANAKA-PtRu/C, NKC-PtRu/C, and KC-PtRu/C 40 (electrolyte: 0.5 M H_2SO_4 + 0.5 M methanol, 30°C, scan rate: 50 mV/s). NKC, non-KOH activated carbon; KC, KOH activated carbon; NHE, normal hydrogen electrode.

CH_3OH + 0.5 M H_2SO_4 solution was scanned at 50 mV/s (Fig. 6). The activity of the platinum electrode catalyst was evaluated according to the peak of the forward current density. In the oxygen absorption session within a range of 0.6–0.8 V, KC-PtRu/C was 1.7 times and 3 times more active than NKC-PtRu/C and TANAKA-PtRu/C, respectively. Meanwhile, all three of the samples showed similar peaks for absorption/desorption area within the range 0.0–0.2 V. KOH activated KC-PtRu/C, which used porous carbon as its support, showed a wider electrochemical catalyst area compared to those of the non-KOH activated NKC-PtRu/C or TANAKA-PtRu/C. This means that KOH activated KC-PtRu/C has the best activity against methanol oxidation.

3.2.4. Onset potential

The onset potential is shown in Table 3. The onset potential of NKC-PtRu/C (0.571 vs. NHE) was higher than that of PtRu/C (0.543V vs. NHE). The potentials were examined and found to decrease in the order NKC-PtRu/C > TANAKA-PtRu/C > KC-PtRu/C.

These results suggest that mesoporous carbon produced by KOH activation affects the catalyst activity [13]; therefore, KC-PtRu/C (0.7232 cm^3/g), of which the mesoporous structure is relatively wide, has a lower onset potential than that of NKC-PtRu/C (0.1043 cm^3/g), which has a smaller mesoporous structure.

4. Conclusions

In this research, PtRu was synthesized using the impregnation method and its support was produced using refined, heat-treated needle coke. We examined the anisotropic structure with a polarization microscope. After the activation of KOH, the sample of KC-PtRu/C (2560.6 m^2/g), into which Pt-Ru catalyst has been loaded, showed a wider specific area than that of NKC-PtRu/C (101.1 m^2/g), which is a non-KOH activated, Pt-Ru loaded sample. In it, an increased number of mesopores was observed. Changes of the XRD pattern at the 26° carbon peak, suggest that the KOH activation brought relevant changes to the structure, which led to an increase of the metal crystallizability. We confirmed through EDS analysis of the precursor that this reduction had been accomplished at the intended Pt/Ru ratio. Through ECSA examination with CV and CO stripping, we confirmed that KC-PtRu/C has a wider effective area than those of the other catalysts. In the methanol oxidation reaction, KC-PtRu showed a higher currency density that those of the other two catalysts (NKC-PtRu/C, TANAKA-PtRu/C). The lowest onset potential was observed for KC-PtRu/C.

Conflict of Interest

No potential conflict of interest relevant to this article was reported.

Acknowledgements

This work was conducted under the framework of the Research and Development Program of the Korea Institute of Energy Research (KIER) (B6-2420-03) and the New & Renewable Energy R&D Program (2012T100201695) of the Korea Institute of Energy Technology Evaluation and Planning (KETEP).

References

[1] Rauhe BR, McLarnon FR, Cairns EJ. Direct anodic oxidation of methanol on supported platinum/uuthenium catalyst in aqueous cesium carbonate. J Electrochem Soc, **142**, 1073 (1995). http://dx.doi.org/10.1149/1.2044547.

[2] Jung DH, Hong SH, Peck DH, Song RH, Shin DR, Kim HN. Development of two-layer electrode for direct methanol fuel cell. J Korean Electrochem Soc, **6**, 68 (2003). http://dx.doi.org/10.5229/JKES.2003.6.1.068.

[3] Ren X, Zelenay P, Thomas S, Davey J, Gottesfeld S. Recent advances in direct methanol fuel cells at Los Alamos National Laboratory. J Power Sources, **86**, 111 (2000). http://dx.doi.org/10.1016/S0378-7753(99)00407-3.

[4] Jeong KJ, Miesse CM, Choi JH, Lee J, Han J, Yoon SP, Nam SW, Lim TH, Lee TG. Fuel crossover in direct formic acid fuel cells. J Power Sources, **168**, 119 (2007). http://dx.doi.org/10.1016/j.jpowsour.2007.02.062.

[5] Cacciola G, Antonucci V, Freni S. Technology up date and new strategies on fuel cells. J Power Sources, **100**, 67 (2001). http://

dx.doi.org/10.1016/S0378-7753(01)00884-9.

[6] Jung DH, Jung JH, Hong SH, Peck DH, Shin DR, Kim E. Characteristics of Pt-Ru catalyst supported on activated carbon for direct methanol fuel cell. Carbon Lett, **4**, 121, (2003).

[7] Lee JS, Han KI, Park SO, Kim HN, Kim H. Performance and impedance under various catalyst layer thicknesses in DMFC. Electrochim Acta, **50**, 807 (2004). http://dx.doi.org/10.1016/j.electacta.2004.01.116.

[8] Pak C, Lee SJ, Lee SA, Chang H. The effect of two-layer cathode on the performance of the direct methanol fuel cell. Korean J Chem Eng, **22**, 214 (2005). http://dx.doi.org/10.1007/BF02701487.

[9] Baeck SH, Choi KS, Jaramillo TF, Stucky GD, McFaland EW. Enhancement of photocatalytic and electrochromic properties of electrochemically fabricated mesoporous WO_3 thin films. Adv Mater, **15**, 1269 (2003). http://dx.doi.org/10.1002/adma.200304669.

[10] Nam KD, Kim SK, Lim SY, Peck DH, Lee BR, Jung DH. Preparation of porous carbon fiber by using MgO powder and its characteristics of catalysts for fuel cell. Korean Chem Eng Res, **46**, 1142 (2008).

[11] Ryoo R, Joo SH, Kruk M, Jaroniec M. Ordered mesoporous carbons. Adv Mater, **13**, 677 (2001). http://dx.doi.org/10.1002/1521-4095(200105)13:9<677::AID-ADMA677>3.3.CO;2-3.

[12] Chai G, Yoon SB, Kang S, Choi JH, Sung YE, Ahn YS, Kim HS, Yu JS. Ordered uniform porous carbons as a catalyst support in a direct methanol fuel cell. Electrochim Acta, **50**, 823 (2004). http://dx.doi.org/10.1016/j.electacta.2003.11.041.

[13] Qiao W, Yoon SH, Mochida I. KOH activation of needle coke to develop activated carbons for high-performance EDLC. Energy Fuels, **20**, 1680 (2006). http://dx.doi.org/ 10.1021/ef050313l.

[14] Marsh H, Crawford D, O'Drady TM, Wennerberg A. Carbons of high surface area: a study by adsorption and high resolution electron microscopy. Carbon, **20**, 419 (1982). http://dx.doi.org/10.1016/0008-6223(82)90042-2.

[15] Otawa T, Tanibata R, Itoh M. Production and adsorption characteristics of MAXSORB: high-surface-area active carbon. Gas Sep Purif, **7**, 241 (1993). http://dx.doi.org/10.1016/0950-4214(93)80024-Q.

[16] Lillo-Ródenas MA, Lozano-Castelló D, Cazorla-Amorós D, Linares-Solano A. Preparation of activated carbons from Spanish anthracite: II. activation by NaOH. Carbon, **39**, 751 (2001). http://dx.doi.org/10.1016/S0008-6223(00)00186-X.

[17] Mochida I, Fujimoto K, Oyama T. Chemistry and Physics of Carbon, Marcel Decker, New York (1994).

[18] Chou KS, Ren CY. Synthesis of nanosized silver particles by chemical reduction method. Mater Chem Phys, **64**, 241 (2000). http://dx.doi.org/10.1016/S0254-0584(00)00223-6.

[19] Coasne B, Gubbins KE, Pellenq RJM. A grand canonical Monte Carlo study of adsorption and capillary phenomena in nanopores of various morphologies and topologies: testing the BET and BJH characterization methods. Part Part Syst Charact, **21**, 149 (2004). http://dx.doi.org/10.1002/ppsc.200400928.

[20] Han DM, Guo ZP, Zeng R, Kim CJ, Meng YZ, Liu HK. Multi-walled carbon nanotube-supported Pt/Sn and Pt/Sn/PMo_{12} electrocatalysts for methanol electro-oxidation. Int J Hydrogen Energy, **34**, 2426 (2009). http://dx.doi.org/10.1016/j.ijhydene.2008.12.073.